

# An information theory based search for homogeneity on the largest accessible scale

Suman Sarkar<sup>\*</sup> and Biswajit Pandey<sup>†</sup>

*Department of Physics, Visva-Bharati University, Santiniketan, Birbhum, 731235, India*

6 September 2018

## ABSTRACT

We analyze the SDSS DR12 quasar catalogue to test the large-scale smoothness in the quasar distribution. We quantify the degree of inhomogeneity in the quasar distribution using information theory based measures and find that the degree of inhomogeneity diminishes with increasing length scales which finally reach a plateau at  $\sim 250 h^{-1}$  Mpc. The residual inhomogeneity at the plateau is consistent with that expected for a Poisson point process. Our results indicate that the quasar distribution is homogeneous beyond length scales of  $250 h^{-1}$  Mpc.

**Key words:** methods: numerical - galaxies: statistics - cosmology: theory - large scale structure of the Universe.

## 1 INTRODUCTION

The assumption that the Universe is statistically homogeneous and isotropic on sufficiently large scales is fundamental to modern cosmology. Our current understanding of the Universe comes from the vast amount of cosmological observations which are hard to interpret without relying on this assumption. Therefore it is important to verify this assumptions using various observations. There are a multitude of evidences favouring isotropy such as the isotropy of the CMBR (Penzias & Wilson 1965; Smoot et al. 1992; Fixsen et al. 1996), isotropy in angular distributions of radio sources (Wilson & Penzias 1967; Blake & Wall 2002), isotropy in the X-ray background (Peebles 1993; Wu et al. 1999; Scharf et al. 2000), isotropy of Gamma-ray bursts (Meegan et al. 1992; Briggs et al. 1996), isotropy in the distribution of galaxies (Marinoni et al. 2012; Alonso et al. 2015), isotropy in the distribution of supernovae (Gupta & Saini 2010; Lin et al. 2016) and isotropy in the distribution of neutral hydrogen (Hazra & Shafieloo 2015). But the local isotropy around us alone is not sufficient to assure large-scale statistical homogeneity. One requires to combine the local isotropy with the Copernican principle to infer the large-scale statistical homogeneity of the Universe. The Copernican principle states that we do not occupy a special location in the Universe which itself requires validation. One can infer the large-scale statistical homogeneity from local isotropy only when it is assured around each and every point in the Universe. So it is not straightforward to

infer large-scale statistical homogeneity of the Universe from the local isotropy.

A large number of studies (Martinez & Coles 1994; Borgani 1995; Guzzo 1997; Cappi et al. 1998; Bharadwaj et al. 1999; Pan & Coles 2000; Yadav et al. 2005; Hogg et al. 2005; Sarkar et al. 2009; Scrimgeour et al. 2012; Nadathur 2013; Pandey & Sarkar 2015; Pandey & Sarkar 2016) find that the galaxy distribution behaves like a fractal on small scales but on large-scale the Universe is homogeneous. Most of these studies claim to have found a transition to homogeneity on scales  $70 - 150 h^{-1}$  Mpc. Contrary to these claims a number of studies (Pietronero 1987; Coleman & Pietronero 1992; Amendola & Palladino 1999; Joyce et al. 1999; Sylos Labini et al. 2007, 2009; Sylos Labini 2011) reported multi-fractal behaviour on different length scales without any transition to homogeneity out to the scale of the survey. The results from these studies clearly indicates that there is no clear consensus in this issue yet. There would be a major paradigm shift in cosmology if the assumption of cosmic homogeneity is ruled out with high statistical significance by multiple data sets.

The most important implication of inhomogeneities comes from the averaging problem in General Relativity through their effect on the large scale dynamics known as backreaction mechanism. The backreaction mechanism is known to cause a global cosmic acceleration without any additional dark energy component (Buchert & Ehlers 1997; Schwarz 2002; Kolb et al. 2006; Buchert 2008; Ellis 2011).

The Sloan Digital Sky Survey (SDSS) (York et al. 2000) is the largest and finest galaxy redshift survey todate. The quasars are the brightest class of objects known as Active

<sup>\*</sup> E-mail:sumansarkar.rs@visva-bharati.ac.in

<sup>†</sup> E-mail: biswap@visva-bharati.ac.in

Galactic Nuclei (AGN). The high luminosities of quasars allow them to be detected out to larger distances. The SDSS DR12 quasar catalogue provides us an unique opportunity to test the assumption of cosmic homogeneity on the largest accessible scale due to its enormous volume coverage. The presence of large quasar groups (LQG) in the quasar distribution is known for quite some time. Clowes et al. (2013) identified a huge LQG with characteristic size  $\sim 500 h^{-1}$  Mpc at  $z \sim 1.3$  in the DR7 quasar catalogue and claimed that this structure is incompatible with large-scale homogeneity indicating possible violation of the cosmological principle. A number of subsequent studies (Nadathur 2013; Marinello et al. 2016) pointed out some flaws in interpreting LQGs as structures. However if such structures really exist then they owe an explanation. In the present study we test the large-scale homogeneity in the SDSS DR12 catalogue using information theory based methods (Pandey 2013; Pandey & Sarkar 2016). We do not address the LQGs separately but the presence of any such structures in the quasar distribution are clearly expected to boost the signal of inhomogeneity up to noticeably larger length scales.

Throughout our work, we have used the flat  $\Lambda$ CDM cosmology with  $\Omega_m = 0.3$ ,  $\Omega_\Lambda = 0.7$  and  $h = 1$ .

A brief outline of the paper follows. In section 2 we describe the method of analysis followed by a description of the data in section 3. We present the results and conclusions in section 4.

## 2 METHOD OF ANALYSIS

Our analysis is based on a method proposed by (Pandey 2013) and its extension (Pandey & Sarkar 2016) which used the Shannon entropy (Shannon 1948) to study inhomogeneities in a 3D distribution. It gives a measure of the average amount of information required to describe a random variable. The Shannon entropy for a discrete random variable  $X$  with  $n$  outcomes  $\{x_i : i = 1, \dots, n\}$  is a measure of uncertainty denoted by  $H(X)$  defined as,

$$H(X) = - \sum_{i=1}^n p(x_i) \log p(x_i) \quad (1)$$

where  $p(x)$  is the probability distribution of the random variable  $X$ .

We first embed the quasar distribution in a  $d h^{-1}$  Mpc  $\times$   $d h^{-1}$  Mpc  $\times$   $d h^{-1}$  Mpc three dimensional rectangular grid which divides the entire survey region into a number of regular cubic voxels. We then identify the voxels which lie partly or completely outside the survey region and discard them to avoid any spurious effects from the boundary. Only the voxels which are fully inside the survey region are retained for the analysis. The grid size  $d$  is varied within a suitable range and each choice of  $d$  result into a different number of voxels and quasars within the survey region. Let  $N_d$  be the number of voxels with grid size  $d$  and  $n_i$  be the number of quasars inside the  $i^{th}$  voxel. Now if we randomly pick up a quasar it can reside only in one of the  $N_d$  voxels i.e. there are  $N_d$  possible outcomes as for the position of this given quasar and the probability of finding the aforementioned quasar in voxel  $i$  is given by,  $f_{i,d} = \frac{n_i}{\sum_{i=1}^{N_d} n_i}$  with the constraint  $\sum_{i=1}^{N_d} f_{i,d} = 1$ .

We denote the outcome of the experiment with a random variable  $X_d$  and the Shannon entropy associated with the random variable  $X_d$  can be written as,

$$\begin{aligned} H_d &= - \sum_{i=1}^{N_d} f_{i,d} \log f_{i,d} \\ &= \log \left( \sum_{i=1}^{N_d} n_i \right) - \frac{\sum_{i=1}^{N_d} n_i \log n_i}{\sum_{i=1}^{N_d} n_i} \end{aligned} \quad (2)$$

Where the base of the logarithm is arbitrary and we choose it to be 10.

We use three different measures of inhomogeneity based on the Shannon entropy defined in Equation 2 and describe them in the following subsections.

### 2.1 Relative Entropy and Entropy Deficit

The probability of finding a quasar in the  $i^{th}$  voxel  $f_{i,d}$  will have the same value  $\frac{1}{N_d}$  for all the voxels when  $n_i$  become the same for all of them. This is an ideal situation when each of the  $N_d$  voxels available contain exactly the same number of quasars within them. This maximizes the Shannon entropy to  $(H_d)_{max} = \log N_d$  for grid size  $d$ . We define the relative Shannon entropy as the ratio of the entropy of a random variable  $X_d$  to the maximum possible entropy  $(H_d)_{max}$  associated with it. The relative Shannon entropy  $\frac{H_d}{(H_d)_{max}}$  for any grid size  $d$  quantifies the degree of uncertainty in the knowledge of the random variable  $X_d$ . Equivalently  $1 - \frac{H_d}{(H_d)_{max}}$  quantifies the residual information and can be treated as a measure of inhomogeneity. The fact that quasars are not residing in any particular voxel and rather are distributed across the available voxels with different probabilities acts as the source of information. If all the quasars would have been residing in one particular voxel leaving the rest of them as empty then there would be no uncertainty at all making  $H_d = 0$  or  $1 - \frac{H_d}{(H_d)_{max}} = 1$ . This fully determined hypothetical situation corresponds to maximum inhomogeneity. On the other hand when all the  $N_d$  voxels are populated with equal probabilities it would be most uncertain to decide which particular voxel a randomly picked quasar belongs to. This maximizes the information entropy to  $H_d = \log N_d$  turning  $1 - \frac{H_d}{(H_d)_{max}} = 0$ .

As  $H_d = (H_d)_{max}$  represents a homogeneous distribution we define the entropy deficit  $(H_d)_{max} - H_d$  to quantify the deviation of the distribution from uniformity. Clearly dividing the entropy deficit by  $(H_d)_{max}$  provides the relative Shannon entropy.

### 2.2 Kullback-Leibler divergence

Alternatively one can measure the inhomogeneity by using the Kullback-Leibler (KL) divergence or information divergence (Kullback & Leibler 1951; Hosoya et al. 2004; Li et al. 2012). In information theory KL divergence is used to measure the difference between two probability distributions  $p(x)$  and  $q(x)$ .

$$D_{KL}(p|q) = \sum_i p(x_i) \log \frac{p(x_i)}{q(x_i)} \quad (3)$$

Let  $f_{Di}$  be the distribution corresponding to the data

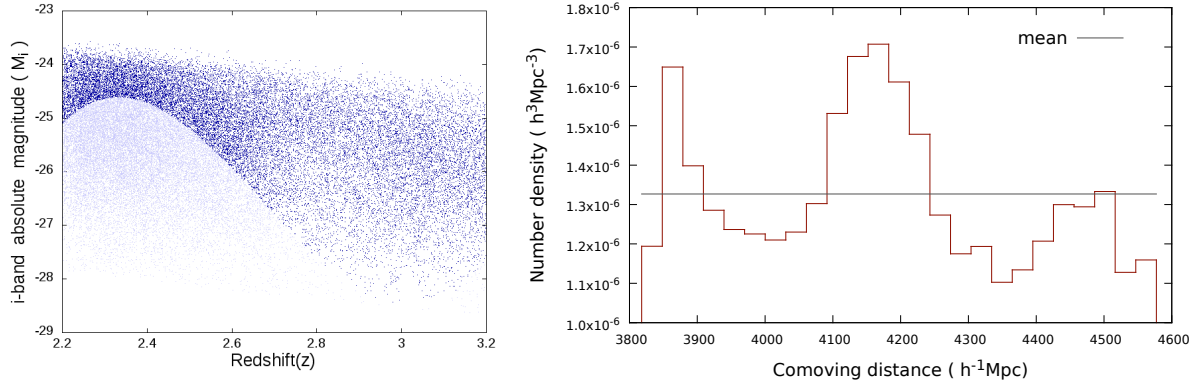


**Figure 1.** The left panel shows the SDSS quasars in the redshift-absolute magnitude plane. The upper region and the lower region in this panel represent the selected and discarded quasars respectively. The right panel shows the comoving number density of quasars as a function of radial distance  $r$ . We compute the density in shells of uniform thickness  $30.73 h^{-1}$  Mpc in the radial direction.

for which homogeneity is to be tested and  $f_{Ri}$  be the distribution for a homogeneous and isotropic Poisson random distribution where both of the distributions occupy same 3D volume with identical geometry and are represented by same number of points.

The KL divergence between the actual and random data is then given by,

$$D_{KL}(D|R) = \frac{(\sum_i n_{Di} \log n_{Di} - \sum_i n_{Di} \log n_{Ri})}{\sum_i n_{Di}} - \log \frac{\sum_i n_{Di}}{\sum_i n_{Ri}} \quad (4)$$

where  $n_{Di}$  and  $n_{Ri}$  are the counts in the  $i^{th}$  voxel for actual data and random data respectively. We use natural logarithm in Equation 4.

### 3 DATA

#### 3.1 SDSS DR12 QUASAR SAMPLE

We use the SDSS DR12 quasar catalog which includes 297301 quasars. The data is downloaded from the link <http://www.sdss.org/dr12/algorithms/boss-dr12-quasar-catalog>. The quasar target selection is described by Ross et al. (2012) and the data is described by Pâris et al. (2014). We first exclude the objects with a ZWARNING value that calls into question the accuracy of their redshift determination. We apply the criteria ZWARNING = 0 (Bolton et al. 2012) and then set UNIFORM  $\geq 1$  to identify a homogeneously selected sample of quasars. This provides the CORE targets selected using XDQSO technique after chunk 12 (Bovy et al. 2011) and also those which would have been selected by XDQSO if it had been the core algorithm prior to chunk 12. We apply further cuts in g-band PSF magnitude  $g \leq 22.0$  and r-band PSF magnitude  $\leq 21.85$  (Ross et al. 2012) to get 117882 quasars with XDQSO probability greater than 0.424. We then construct our quasar sample covering a contiguous region of right ascension  $150^\circ \leq \alpha \leq 240^\circ$  and declination  $0^\circ \leq \delta \leq 60^\circ$  in the redshift range  $2.2 \leq z \leq 3.2$ . The resulting quasar sample does not have a uniform number density in the entire redshift range. We find that constructing a volume limited

sample of quasars from this data results into a sample with a very poor number density. So to construct a quasar sample we use a cut  $M_i \geq M_{lim}(z)$  in the i-band absolute magnitude which varies with redshift. We describe  $M_{lim}(z)$  with a polynomial as  $M_{lim}(z) = az^3 + bz^2 + cz + d$  where  $a, b, c$  and  $d$  are the coefficients to be determined. We constrain these coefficients so as to produce a quasar sample with a near uniform comoving number density. We find that the coefficients  $a = 24.206, b = -194.325, c = 511.413, d = -467.422$  produces a quasar sample consisting of 24213 quasar which has less than 30% variation (Figure 1) in number density around the mean in the entire redshift range. The sample has a volume of  $1.83 \times 10^{10} (h^{-1} \text{Mpc})^3$  with a linear extent of  $759.32 h^{-1}$  Mpc in the radial direction. The mean number density of the quasar sample is  $1.326 \times 10^{-6} h^3 \text{Mpc}^{-3}$ .

#### 3.2 RANDOM SAMPLES

We construct 30 mock random samples from homogeneous and isotropic 3D Poisson point processes. The mock random samples contain exactly the same number of points as there are quasars in our sample and are distributed within a region which have the same geometry as the quasar sample.

### 4 RESULTS AND CONCLUSIONS

We present our results in Figure 2. In top left and middle left panel of the Figure 2 we show respectively the variation of  $1 - \frac{H_d}{(H_d)_{max}}$  and  $(H_d)_{max} - H_d$  with increasing grid sizes for the quasar sample and its random mock counterparts. Both the quasar sample and the random samples have a mean inter-particle separation of  $91 h^{-1}$  Mpc and they are hardly distinguishable below this length scale but as the grid size increases the differences become evident. In both of the plots we find that the quasar sample has a higher information content than the Poisson samples throughout the entire length scale ranges due to the gravitational clustering. However the differences diminish with increasing length scales and at  $\sim 250 - 300 h^{-1}$  Mpc the results for the Poisson samples lies within  $1 - \sigma$  errorbars of the same for the quasar sample. The residual inhomogeneities beyond  $250 h^{-1}$  Mpc

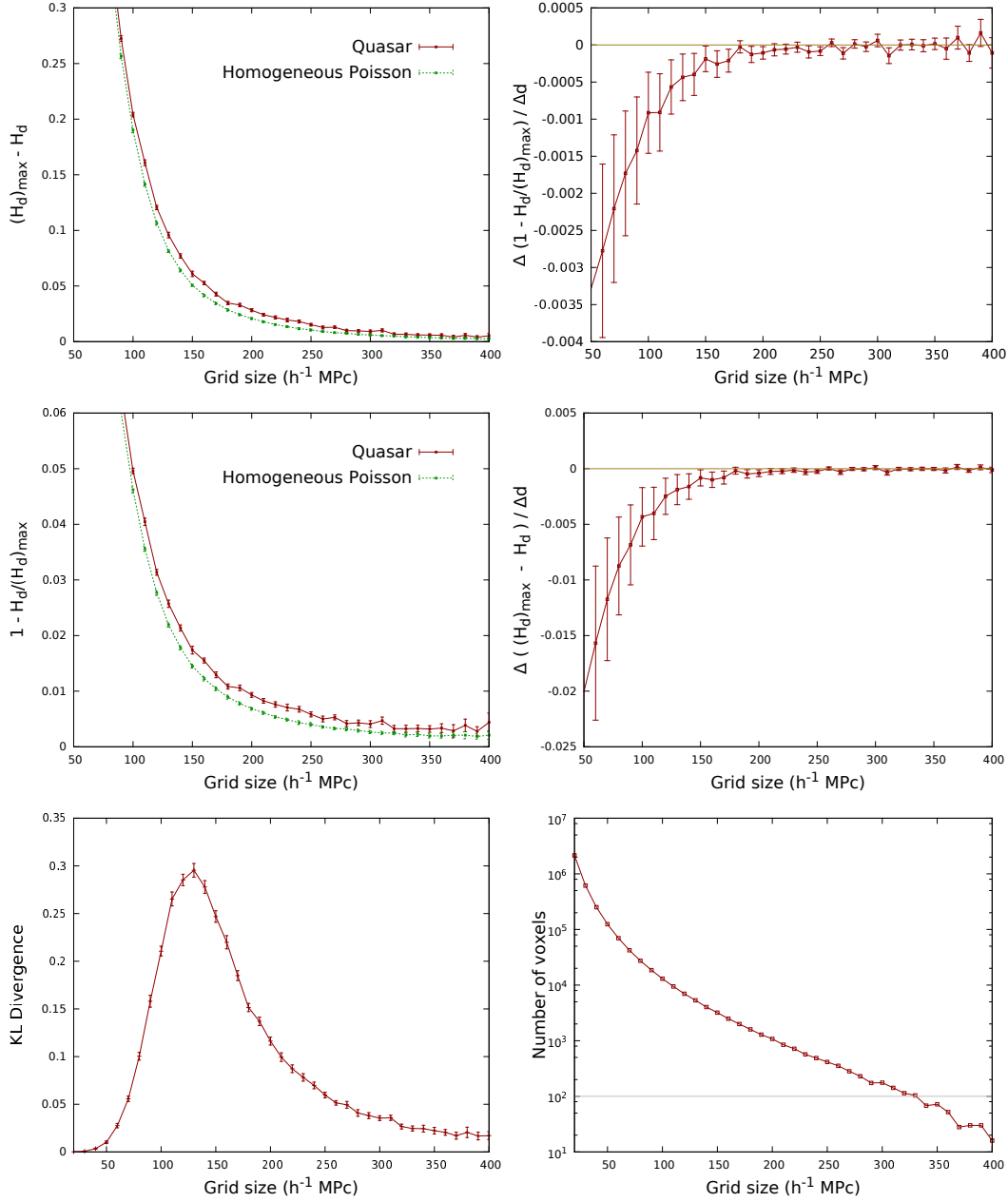


**Figure 2.** The top left and middle left panels show  $1 - \frac{H_d}{(H_d)_{max}}$  and  $(H_d)_{max} - H_d$  as a function of length scales respectively. The slopes of the respective quantities in the quasar sample are shown in the top right and middle right panels. The bottom left panel shows the KL divergence as a function of length scales and the bottom right panel shows the number of voxels available at each length scales. The errorbars for the quasar sample are obtained from 30 bootstrap samples and the errorbars for the Poisson samples are obtained from 30 Monte Carlo realizations of the same.

are consistent with what one would expect for a homogeneous Poisson point process. We show the rates of change of  $1 - \frac{H_d}{(H_d)_{max}}$  and  $(H_d)_{max} - H_d$  in the quasar sample with increasing length scales in the top right and middle right panels of Figure 2 respectively. We find that the rates of change for both of the measures in the quasar sample diminish nearly to zero with tiny errorbars at  $\sim 250 h^{-1}$  Mpc. In the bottom left panel of Figure 2 we show the KL divergence measure as a function of length scales in the quasar sample. The KL divergence also indicates that the inhomogeneities diminish with increasing length scales finally

reaching a plateau at  $\sim 250 - 300 h^{-1}$  Mpc. However it is worth mentioning here that though the entropy is sensitive to the higher order moments of a distribution it may not capture the signatures of the full hierarchy of correlation functions. A Minkowski Functional analysis of SDSS LRGs by Wiegand et al. (2014) find significant deviations from the  $\Lambda$ CDM mock catalogues on scales of  $500 h^{-1}$  Mpc.

It has been suggested that the quasars inhabit dark matter halos of constant mass  $\sim 2 \times 10^{12} h^{-1} M_\odot$  from redshifts  $z \sim 2.5$  (the peak of quasar activity) to  $z \sim 0$  and their large scale linear bias evolves from  $b = 3$  at  $z \sim 2.2$

to  $b = 1.38$  at  $z \sim 0.5$  (Shen et al. 2013; Ross et al. 2009; Geach et al. 2013). Our quasar sample extends from  $z = 2.2$  to  $z = 3.2$  for which we expect a large scale linear bias of  $\gtrsim 3$ . As the quasars inhabit rarer high density peaks one would expect the quasar sample to be homogeneous on even larger scale than the SDSS main galaxy sample and the LRG sample. Our result is consistent with our earlier studies on the SDSS main galaxy sample (Pandey & Sarkar 2015) and the LRG sample (Pandey & Sarkar 2016) for which we find a transition scale to homogeneity at  $\sim 150 h^{-1}$  Mpc.

It may be noted here that there are 414 independent voxels (bottom right panel of Figure 2) at grid size of  $250 h^{-1}$  Mpc and each voxel is expected to host  $\sim 21$  quasars provided the distribution is homogeneous beyond this length scale. This number is certainly very small due to the small number density of the quasar sample. Further we can not have access to spatial hypersurface of constant time. So any analysis of homogeneity on large scales would unavoidably incorporate some signatures of the time evolution. Despite these difficulties it is interesting to note the degree of homogeneity in the quasar sample beyond a length scale of  $250 h^{-1}$  Mpc. Last but not the least we prepare 4 different quasar samples with different set of values for the coefficients ( $a, b, c, d$ ) used to define the limiting magnitudes at different redshifts. Irrespective of our choice we find the same transition scale to homogeneity in each of these quasar samples. We finally conclude that the SDSS quasar distribution is homogeneous beyond  $250 h^{-1}$  Mpc, for the information theoretic measures employed in this paper.

## 5 ACKNOWLEDGEMENT

The authors would like to thank the SDSS team for making the data publicly available. B.P. would like to acknowledge IUCAA, Pune and CTS, IIT Kharagpur for the use of its facilities for the present work.

## REFERENCES

- Alonso, D., Salvador, A. I., Sánchez, F. J., et al. 2015, MNRAS, 449, 670
- Amendola, L., & Palladino, E. 1999, ApJ Letters, 514, L1
- Bharadwaj, S., Gupta, A. K., & Seshadri, T. R. 1999, A&A, 351, 405
- Bolton, A. S., Schlegel, D. J., Aubourg, É., et al. 2012, AJ, 144, 144
- Borgani, S. 1995, Physics Reports, 251, 1
- Bovy, J., Hennawi, J. F., Hogg, D. W., et al. 2011, ApJ, 729, 141
- Blake, C., & Wall, J. 2002, Nature, 416, 150
- Briggs, M. S., Paciasas, W. S., Pendleton, G. N., et al. 1996, ApJ, 459, 40
- Buchert, T., & Ehlers, J. 1997, A&A, 320, 1
- Buchert, T. 2008, General Relativity and Gravitation, 40, 467
- Cappi, A., Benoist, C., da Costa, L. N., & Maurogordato, S. 1998, A&A, 335, 779
- Coleman, P. H., Pietronero, L. 1992, Physics Reports, 213, 311
- Clowes, R. G., Harris, K. A., Raghunathan, S., et al. 2013, MNRAS, 429, 2910
- Ellis, G. F. R. 2011, Classical and Quantum Gravity, 28, 164001
- Fixsen, D. J., Cheng, E. S., Gales, J. M., et al. 1996, ApJ, 473, 576
- Geach, J. E., Hickox, R. C., Bleem, L. E., et al. 2013, ApJ Letters, 776, L41
- Gupta, S., & Saini, T. D. 2010, MNRAS, 407, 651
- Guzzo, L. 1997, New Astronomy, 2, 517
- Hazra, D. K., & Shafieloo, A. 2015, JCAP, 11, 012
- Hogg, D. W., Eisenstein, D. J., Blanton, M. R., Bahcall, N. A., Brinkmann, J., Gunn, J. E., & Schneider, D. P. 2005, ApJ, 624, 54
- Hosoya, A., Buchert, T., & Morita, M. 2004, Physical Review Letters, 92, 141302
- Joyce, M., Montuori, M., & Labini, F. S. 1999, ApJ Letters, 514, L5
- Kullback, S. & Leibler, R. A. 1951, The Annals of Mathematical Statistics, 22, 79
- Kolb, E. W., Matarrese, S., & Riotto, A. 2006, New Journal of Physics, 8, 322
- Li, N., Buchert, T., Hosoya, A., Morita, M., & Schwarz, D. J. 2012, Physical Review D, 86, 083539
- Lin, H.-N., Wang, S., Chang, Z., & Li, X. 2016, MNRAS, 456, 1881
- Martinez, V. J., & Coles, P. 1994, ApJ, 437, 550
- Marinello, G. E., Clowes, R. G., Campusano, L. E., et al. 2016, arXiv:1603.03260, Accepted in MNRAS
- Marinoni, C., Bel, J., & Buzzi, A. 2012, JCAP, 10, 036
- Meegan, C. A., Fishman, G. J., Wilson, R. B., et al. 1992, Nature, 355, 143
- Nadathur, S. 2013, MNRAS, 434, 398
- Pan, J., & Coles, P. 2000, MNRAS, 318, L51
- Pandey, B. 2013, MNRAS, 430, 3376
- Pandey, B. & Sarkar, S. 2015, MNRAS, 454, 2647
- Pandey, B., & Sarkar, S. 2016, MNRAS, 460, 1519
- Pâris, I., Petitjean, P., Aubourg, É., et al. 2014, A&A, 563, A54
- Penzias, A. A., & Wilson, R. W. 1965, ApJ, 142, 419
- Peebles, P. J. E. 1993, Principles of Physical Cosmology. Princeton, N.J., Princeton University Press, 1993
- Pietronero, L. 1987, Physica A Statistical Mechanics and its Applications, 144, 257
- Ross, N. P., Shen, Y., Strauss, M. A., et al. 2009, ApJ, 697, 1634
- Ross, N. P., Myers, A. D., Sheldon, E. S., et al. 2012, ApJS, 199, 3
- Sarkar, P., Yadav, J., Pandey, B., & Bharadwaj, S. 2009, MNRAS, 399, L128
- Shannon, C. E. 1948, Bell System Technical Journal, 27, 379-423, 623-656
- Scharf, C. A., Jahoda, K., Treyer, M., et al. 2000, ApJ, 544, 49
- Scrimgeour, M. I., Davis, T., Blake, C., et al. 2012, MNRAS, 3412
- Schwarz, D. J. 2002, arXiv:astro-ph/0209584
- Shen, Y., McBride, C. K., White, M., et al. 2013, ApJ, 778, 98
- Smoot, G. F., Bennett, C. L., Kogut, A., et al. 1992, ApJ Letters, 396, L1
- Sylos Labini, F., Vasilyev, N. L., & Baryshev, Y. V. 2007, A&A, 465, 23
- Sylos Labini, F., Vasilyev, N. L., & Baryshev, Y. V. 2009, A&A, 508, 17
- Sylos Labini, F. 2011, Europhysics Letters, 96, 59001
- Wiegand, A., Buchert, T., & Ostermann, M. 2014, MNRAS, 443, 241
- Wilson, R. W., & Penzias, A. A. 1967, Science, 156, 1100
- Wu, K. K. S., Lahav, O., & Rees, M. J. 1999, Nature, 397, 225
- Yadav, J., Bharadwaj, S., Pandey, B., & Seshadri, T. R. 2005, MNRAS, 364, 601
- York, D. G., et al. 2000, AJ, 120, 1579

This paper has been typeset from a  $\text{\TeX}/\text{\LaTeX}$  file prepared by the author.